Numerical investigation on the spark ignition of laminar strained premixed NH$_3$-air flames with CH$_4$ and H$_2$ as co-fuels

Chunkan Yu, Robert Schießl, Ulrich Maas,
Karlsruhe Institute of Technology (KIT),
Karlsruhe, Germany

Detlev Markus, Stefan Essmann, Bo Shu
Physikalische-Technische Bundesanstalt (PTB)
Brauschweig, Germany

1 Introduction

Given the strict political regulations for reducing greenhouse gas (GHG) emissions, efforts have been made to develop the application of renewable energies. Since there are many applications that cannot be fully electrified, e.g., power generation, steel/cement industry, marine and aviation, alternative energy carriers are being investigated. Among the other candidates, ammonia is attracting more attention due to its preferred characteristics such as carbon-free, high energy density, and mature infrastructure for transportation and storage [1]. Additionally, ammonia can be synthesized directly via power-to-ammonia method applying renewable energy sources [2]. Recently, the application scenarios of ammonia as fuel in boilers, internal combustion engines, gas turbines as well as fuel cells have been comprehensively reviewed, along with detailed safety aspects [1]. However, there was no systematical assessment reported in the literature for the ignition energy of ammonia that is essential for the hazards prevention in the practical applications.

A particularly important case for technical applications are mixtures of ammonia with hydrogen (H$_2$) and with methane (CH$_4$) [1]. By-mixing hydrogen to ammonia can be used to enhance the reactivity of ammonia. Also, in technical applications that use NH$_3$, hydrogen often appears as a co-product, and the ignition properties of the ammonia/hydrogen mixtures are important, e.g., to assess possible safety risks by accidental ignition. Similarly, methane, as the main component of natural gas, is a co-fuel candidate for enhancing ammonia combustion. For both H$_2$ and CH$_4$, the knowledge base on ignition properties of their mixtures with NH$_3$ is still scarce.

Although most practical combustion devices are operating under turbulent conditions, the complex interaction between the chemistry and the turbulence complicates the understanding of the whole processes. The laminar flame, on the other hand, provides a suitable flame analysis, which enables us to understand the interaction between the chemistry and the flow conditions.

2   Mathematical Modeling and Numerical Calculation

Our simulations address the question under which conditions an ignition in flows of premixtures of air with methane (CH_4)/ammonia and hydrogen (H_2)/ammonia is successful, i.e., leads to a self-sustaining flame propagation. The dependence of ignition success on ignition source properties, initial mixture composition, and strength of flow is determined. Figure 1 depicts the counterflow configuration modeled by our simulations.
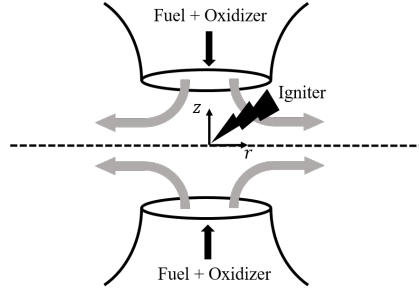

Figure 1: Illustration of a counterflow configuration with an igniter

From two gas inlets, unburned $NH_3/CH_4/H_2$/air mixtures with the same states (temperature T_{ub}, fuel/air equivalence ratio Φ, pressure p) and the same absolute value of velocity v_{ub} emerge and then impinge into each other. A spark igniter centered at $(z = 0, r = 0)$ provides thermal energy to heat up and ignite the gas mixture. In case of successful ignition, a flame in the $r-$plane results. This configuration can be modeled as a one-dimensional system, with the flame-normal coordinate z as spatial variable [3]. The resulting system of partial differential equations (PDE) is a two-parameter formulation, in which two independent parameters (tangential pressure gradient J and radial velocity gradient G) are introduced [3]. This formulation was shown to be applicable to both stationary and non-stationary problems [3].

By considering the spark ignition, there is an additional external ignition energy $\dot{q}_s(z,t)$ appearing in the conservation equation for energy. The $\dot{q}_s(z,t)$ is the provided ignition power density modeled as [4]:

$$\dot{q}_s(z,t) = \begin{cases} \frac{D_s}{\tau_s} \cdot \exp\left[-\left(\frac{z}{\delta_W}\right)^8\right] & (0 \leq t \leq \tau_s), \\ 0 & \text{(otherwise)} \end{cases} \tag{1}$$

where D_s is the energy density (J/m^3) at $z = 0$, and δ_W is the spark width in m. Note that the present work focuses on the effect of the strain rate, gas mixture thermo-kinetic states, spark igniter geometry and spark energy on the spark ignition process. Therefore we simplify the modeling of the external spark energy, assuming that it solely depends on the z-coordinate (symmetry around r-axis). A study of spark ignition in more complex, two dimensional geometries can be found in e.g. [5]. For the considered combustion system (c.f. Fig.1), E_s is the deposited energy per surface and has units of J/m^2, which can be determined as:

$$E_s = \int_{z=-\infty}^{+\infty} \int_{t=0}^{\tau_s} \dot{q}_s(z,t)\mathrm{d}t\mathrm{d}z = 2 \cdot D_s \cdot \delta_W \cdot \Gamma\left(\frac{9}{8}\right) \tag{2}$$

where $\Gamma(\cdot)$ is the gamma function ($\Gamma(9/8) \approx 0.94174$).

The "strength" of the flow is represented by the tangential pressure gradient J, which is constant for a given flow configuration. The strain rate a is related to J by $a = \sqrt{-\frac{J}{\rho_{ub}}}$, where ρ_{ub} is the density of the unburned mixture.

It is assumed that the pressure is spatially and temporally uniform, which corresponds to the low Mach number approximation. As shown in [6], this uniform pressure assumption is a very good approximation

for $\tau_s > 10\mu s$. All substances involved in the flow are treated as ideal gases. The system of PDEs requires initial and boundary conditions for a unique solution. Initially, all the thermo-kinetic states such as temperature ($T(z,t)$) and species concentrations (mass fraction $w_i(z,t)$) are homogeneously distributed through the whole spatial domain. In other words, no spatial gradients of temperature and species concentrations exist:

$$T(z,t=0) = T_{\text{ub}}, \quad w_i(z,t=0) = w_{i,0}. \tag{3}$$

For left boundary, we set the symmetry line ($z = 0$ in Fig.1)y. Neumann boundary conditions are specified for temperature $T(z,t)$ and species concentrations $w_i(z,t)$: $\partial T/\partial z|_{z=0} = 0$, and $\partial w_i/\partial z|_{z=0} = 0$. The velocity is $v = 0$ because it corresponds to the stagnation point.

For right boundary, Dirichlet boundary conditions are specified. Values of temperature $T = T_{\text{ub}}$ and species concentrations $w_i = w_{i,0}$ remain unchanged at any time here. Furthermore, a constant value of the tangential pressure gradient J is specified to define the strain rate.

For a given co-fuel (CH_4 or H_2) of ammonia, the composition of unburned fuel/air mixture is parameterized by the mole fraction α of NH_3 in the fuel, and the fuel/air equivalence ratio Φ. The molar shares of fuel, O_2 and N_2 are given by

$$(1-\alpha)H_2 + \alpha NH_3 + \frac{1}{\Phi}\left(0.5 + \frac{\alpha}{4}\right)(O_2 + \frac{79}{21}N_2)$$

and

$$(1-\alpha)CH_4 + \alpha NH_3 + \frac{1}{\Phi}\left(2 - \frac{5\alpha}{4}\right)(O_2 + \frac{79}{21}N_2)$$

The chemical reactions are treated by a detailed reaction mechanism from [7]. This mechanism is originally developed by Li and co-workers for ammonia/methane/hydrogen mixtures [8] and further improved due to better accuracy following the suggestion by [7]. The numerical computation is performed using the in-house code INSFLA [9], which has been extended to enable the simulation of counterflow flames based on the governing equations proposed in [3]. A detailed transport model including thermal diffusion (Soret effect) is considered [10].

3 Successful and failed ignition

Spark ignition is a complex process which is governed by chemical reaction, convection and diffusion. Furthermore, the supply of energy by the spark and the flow condition (e.g. strain rate) also play a significant role.

The interaction of these processes leads to two qualitative outcomes, namely a failed SI or a successful SI. To distinguish both, Fig.2 shows one representative temperature development of a NH_3/H_2/air combustion system over time and spatial coordinates. The red lines stand for the temperature profiles during SI duration, and the blue lines for those after SI. For both cases, the only difference is the deposited SI energy: for the failed SI $D_s = 310\,\text{kJ/m}^3$, and for a successful SI $D_s = 320\,\text{kJ/m}^3$ (corresponding to the minimum spark ignition energy D_s^{min} for a successful SI). It is obvious that the temperature increases continuously during the SI duration, because the gas mixture is heated up through the spark igniter. After the spark duration time, one obtains:

- a failed SI: as shown in Fig.2(left), if at the steady state the temperature of the whole system is again the same as the initial temperature (homogeneous temperature distribution), or

- a successful SI: as shown in Fig.2(right), if after a certain time we obtain a stable steady burning flame at steady state.
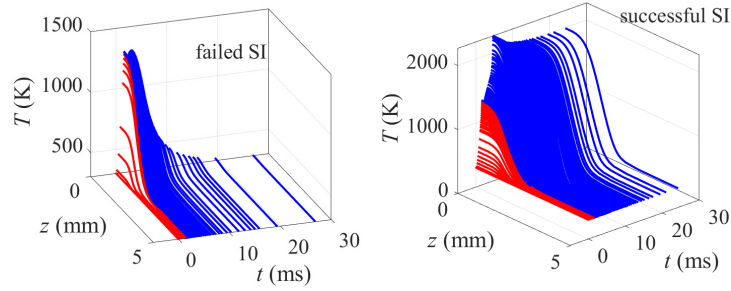
Figure 2: Temporal development of spatial temperature profiles for a failed SI (left) and a successful SI (right). The imposed strain rate is a=100 s^{-1}; spark width δ_W=1 mm; spark duration time τ_s =1.5 ms. Gas mixture: NH$_3$:H$_2$ = 0.9:0.1 with stoichiometric mixture.

4   Results and Discussion

In the following discussion, we will focus on the minimum ignition energy density $D_s^{\min}$ required for a successful ignition. The effect of the spark duration τ_s, the fuel/air equivalence ratio Φ, the amount of added co-fuel (H$_2$ or CH$_4$), the strain rate a and the gas mixture temperature T_{ub} on the $D_s^{\min}$ will be investigated and discussed in detail. In all calculations, the pressure is set to 1 bar and the initial temperature over the whole domain is 298 K. In the spark model a spark width $\delta_W = 1$ mm is used (c.f. Eq.1). This choice is a typical value for technical applications [11–13].

We first investigate the effect of the spark duration τ_s on $D_s^{\min}$. Fig.3 shows the dependence $D_s^{\min}(\tau_s)$ for stoichiometric fuel-air mixtures of ammonia/CH$_4$ and ammonia/H$_2$ fuels.
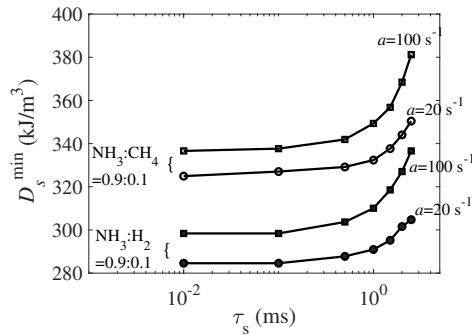

Figure 3: Dependence of $D_s^{\min}$ on different spark duration τ_s for different gas mixture with $\Phi = 1.0$.

It is observed that at very short spark durations (here, 0.01 ms $\leq \tau_s \leq$ 0.1 ms), $D_s^{\min}$ is almost independent of τ_s. In contrast, $D_s^{\min}$ increases strongly with τ_s for τ_s near and above 1 ms. As analyzed in [9], this phenomenon can be explained by considering the competition between the energy dissipation rate caused by heat conductivity and the heat-up rate caused by the external spark energy source:

- at short spark durations, the rate of energy transport out of the spark volume is much smaller than the heat-up rate. Practical all spark ignition energy will therefore be deposited into the spark volume, rather than getting distributed into the ambience during the spark duration. Therefore, the $D_s^{\min}$ almost does not depend on the short spark duration,

- at long spark durations, significant part of the spark energy will get transported out of the spark volume within the duration of the spark. Therefore, more spark energy must be supplied to cre-

ate high temperatures in the spark volume that allow chemical reactions to commence. Larger $D_s^{\min}$ therefore result for longer spark durations.

Fig.4 shows $D_s^{\min}$ as a function of strain rate for different mixtures. We observe the following dependencies:

- $D_s^{\min}$ decreases with increasing content of H_2 or CH_4 in the fuel; This is because the increase of H_2 and CH_4 accelerate the chemical reaction.

- the NH_3/CH_4/air mixture requires higher $D_s^{\min}$ than the NH_3/H_2/air mixture. This is because the NH_3/H_2/air mixture has much higher reaction rate than the NH_3/CH_4/air mixture, which is described in terms of ignition delay times [7, 8].

- the addition of H_2 has a larger effect on the $D_s^{\min}$ than the addition of CH_4. More precise, a decrease of $D_s^{\min}$ by adding H_2 is larger than by adding the same mole content of CH_4 in the ammonia gas. This is mainly because with more addition of H_2 the gas mixtures require higher reaction rate to win over the high molecular diffusivity, where the molecular diffusivity remains almost the same by adding more content of CH_4 in the gas mixture.
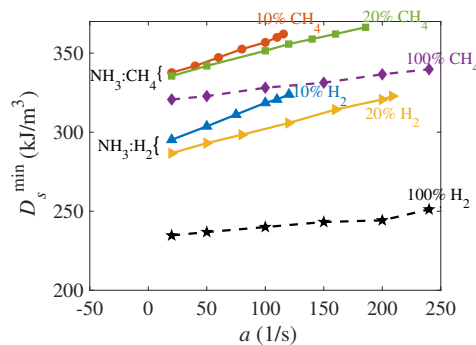

Figure 4: Dependence of $D_s^{\min}$ on strain rate for gas mixtures with different compositions. $\tau_s = 1.5$ ms.

5 Conclusion

The present paper studies the spark ignition properties of ammonia/methane/air and ammonia/hydrogen/air gas mixtures by numerical simulations. Laminar strained premixed flame calculations, which are based on a detailed treatment of chemical reactions and molecular transport, are used to assess the dependence of minimum ignition energy $D_s^{\min}$ on spark properties, strain rate and mixture composition.

It is mainly found that $D_s^{\min}$ is nearly independent of spark duration τ_s at short spark durations, while it increases rapidly with τ_s at larger τ_s. Secondly, flows with higher strain rates require higher $D_s^{\min}$. Furthermore, both for ammonia/H_2 and ammonia/CH_4 mixtures, $D_s^{\min}$ decreases when the content of the co-fuel H_2 or CH_4 is increased. Moreover, with increasing H_2-content, ammonia/H_2 mixtures require higher reaction rates for initiating and maintaining combustion, while ammonia/CH_4 mixtures are not notably affected by this, because the mixture's molecular diffusivity remains almost unchanged by addition of CH_4 to ammonia.

References

[1] A. Valera-Medina, F. Amer-Hatem, A. K. Azad, I. C. Dedoussi, M. De Joannon, R. X. Fernandes, P. Glarborg, H. Hashemi, X. He, S. Mashruk, J. McGowan, C. Mounaim-Rouselle, A. Ortiz-Prado, A. Ortiz-Valera, I. Rossetti, B. Shu, M. Yehia, H. Xiao, and M. Costa, "Review on ammonia as a potential fuel: from synthesis to economics," *Energy Fuels*, vol. 35, no. 9, pp. 6964–7029, 2021.

[2] J. Ikäheimo, J. Kiviluoma, R. Weiss, and H. Holttinen, "Power-to-ammonia in future north european 100% renewable power and heat system," *Int. J. Hydrog. Energy*, vol. 43, no. 36, pp. 17 295–17 308, 2018.

[3] G. Stahl and J. Warnatz, "Numerical investigation of time-dependent properties and extinction of strained methane- and propane-air flamelets," *Combust. Flame*, vol. 85, no. 3-4, pp. 285–299, 1991.

[4] U. Maas, B. Raffel, J. Wolfrum, and J. Warnatz, "Observation and simulation of laser induced ignition processes in O_2-O_3 and H_2-O_2 mixtures," *Proc. Combust. Inst.*, vol. 21, no. 1, pp. 1869–1876, 1988.

[5] M. Thiele, J. Warnatz, and U. Maas, "Geometrical study of spark ignition in two dimensions," *Combust. Theory Model.*, vol. 4, no. 4, p. 413, 2000.

[6] U. Maas and J. Warnatz, "Ignition processes in hydrogen-oxygen mixtures and the influence of the uniform pressure assumption," in *Dynamics of Reactive Systems Part I: Flames; Part II: Heterogeneous Combustion and Applications*, A. L. Kuhl, J. R. Bowen, A. Borisov, and J.-C. Leyer, Eds. Washington DC: American Institute of Aeronautics and Astronautics, 1988, pp. 3–18.

[7] B. Shu, X. He, C. Ramos, R. Fernandes, and M. Costa, "Experimental and modeling study on the auto-ignition properties of ammonia/methane mixtures at elevated pressures," *Proc. Combust. Inst.*, vol. 38, no. 1, pp. 261–268, 2021.

[8] R. Li, A. A. Konnov, G. He, F. Qin, and D. Zhang, "Chemical mechanism development and reduction for combustion of NH_3/H_2/CH_4 mixtures," *Fuel*, vol. 257, p. 116059, 2019.

[9] U. Maas and J. Warnatz, "Ignition processes in hydrogen- oxygen mixtures," *Combust. Flame*, vol. 74, no. 1, pp. 53–69, 1988.

[10] J. O. Hirschfelder, C. F. Curtiss, R. B. Bird, and M. G. Mayer, *Molecular theory of gases and liquids*. Wiley New York, 1964, vol. 165.

[11] P. H. Shu-Yi, A. Khalid, A. Mohamad, B. Manshoor, A. Sapit, I. Zaman, and A. Hashim, "Analysis of spark plug gap on flame development using schlieren technique and image processing," in *IOP Conference Series: Materials Science and Engineering*, vol. 160, no. 1. IOP Publishing, 2016, p. 012044.

[12] K. Kim and O. Askari, "Understanding the effect of capacitive discharge ignition on plasma formation and flame propagation of air–propane mixture," *J. Energy Resour. Technol.*, vol. 141, no. 8, 2019.

[13] O. Baş, M. A. Akar, H. Serin, M. Özcanlı, and E. Tosun, "Variation of spark plug type and spark gap with hydrogen and methanol added gasoline fuel: Performance characteristics," *Int. J. Hydrog. Energy*, vol. 45, no. 50, pp. 26 513–26 521, 2020.